Supporting Information

Non-invasive Spatiotemporal Profiling of the Processes of Impregnation and Drying within Mo/Al$_2$O$_3$ Catalyst Bodies by a Combination of X-ray Absorption Tomography and Diagonal Offset Raman Spectroscopy

Emma K. Gibson[1], Mathijs W. Zandbergen[1], Simon D. M. Jacques[2], Cai Biao[2], Robert J. Cernik[2], Matthew G. O'Brien[1], Marco Di Michiel[3], Bert M. Weckhuysen[1,]*, Andrew M. Beale[1,]*

1 Inorganic Chemistry and Catalysis group, Debye Institute for Nanomaterials Science, Utrecht University, Universiteitsweg 99, 3584 CG Utrecht, The Netherlands

2 The School of Materials, The University of Manchester, Manchester, M13 9PL, UK

3 The European Synchrotron Facility, 6 Rue Jules Horowitz, 38000, Grenoble, France

* To whom correspondence should be addressed: a.m.beale@uu.nl, b.m.weckhuysen@uu.nl

Micro-distributions in a cylindrical catalyst extrudate

Figure S1. A schematic description of the micro-distributions of an active phase in a cylindrical extrudate as observed when bisected.

μ-Absorption-CT and numerical modeling of particle growth

Explanation of μ-Absorption-CT

X-ray micro-tomography (commonly referred to as μ-CT) gives a 2D or 3D x-ray attenuation based upon the transmission of X-rays through a sample:

$$I = I_0 e^{-\mu t}$$

Where I_0 is the incident beam intensity, μ is the absorption coefficient and t is the path length. In 3D μ-CT, the raw data consists of a projection set which is a series of 2D images (wherein each pixel is a measurement of I) of the projected measured intensity at a series of angles. A reconstructed volume can be found by tomographic reconstruction where the volume elements (voxels) each contain a reconstructed absorption coefficient (μ) having units of cm^{-1}.

The time-resolved experiments approximate to a closed system: the sample does not move outside of the sampled region and consequently all of the chemicals within the system remain inside the field of view. The only losses that occur can be by volatilisation of material to the atmosphere. In the systems studied the only losses occurring are water loss through evaporation. The 2D time series maps presented are taken from a time series of 3D reconstructed volumes. They are presented such that the colour quantity represents the value of μ, with a common colour scale bar indicating the specific values.

The alumina catalyst body is a microporous structure containing large and small voids. It typically has μ values ~ 0.6 cm^{-1}. Saturating with water leads to values of up to ~ 1.0 cm^{-1}. Adding a metal solution, e.g. the 1.3 M AHM gives significantly greater values. When Mo (the dominant species in terms of absorption) localises due to the chemical solution gradients or precipitation, even larger values of μ are observed. We can then directly observe the migration of the metal species in the closed systems under study.

Experimental

The sample was first mounted and aligned using the goniometer. μ-Absorption-CT data were then recorded under dry pre-loaded conditions. In some cases μ-Absorption-CT under wet conditions (water only) was also performed to assess the water contribution before the sample was allowed to dry. The sample would then be taken off (goniometer intact) before loading (1.3 M [Mo] ammonium heptamolybdate solution at pH 5) and shaking (shaken as the whole unit i.e. goniometer + sample). The sample plus goniometer would then be remounted and the timed series of μ-Absorption-CT performed. In all cases there was a slight but significant shift in sample before and after loading. One should also note that a small tilt of the sample occurred during the run; presumably because of the glue failing.

Results

A segmentation process was performed on the final X-ray μ-Absorption-CT volume data set; separating parts of the image based on intensity (μ) and connectivity. Pixels were grouped together if they were connected and labeled as one volume (hotspot). A threshold of μ > 3.2 was used to discriminate between hotspots and background Mo concentration. Information on the connected regions can be extracted, such as volume by adding the number of connected pixels, mass from the total value of μ in the connected pixels, centre-of-mass location and approximate shape. A list of particles, locations and sizes were generated for 1007 particles and sorted according to particle size, those having volumes between 163 to 2783 pixels were chosen for further analysis (500 particles). Particles were eliminated from this data set if they were located

outside the rectangle shown in Figure S2, as they were deemed too close to the top and bottom of the extrudate and so in a region of non-uniform impregnation. As is clear from Figure S2 the impregnation was not uniform along the z-axis of the extrudate and even in the subsection chosen there is a concentration gradient. Particles which underwent coalescence were also rejected from the analysis. Coalescence was determined by visual inspection of the volume time profiles of the remaining particles; those which showed a jump in the apparent growth curve were considered to have undergone coalescence with a neighbouring particle and were rejected from the analysis.
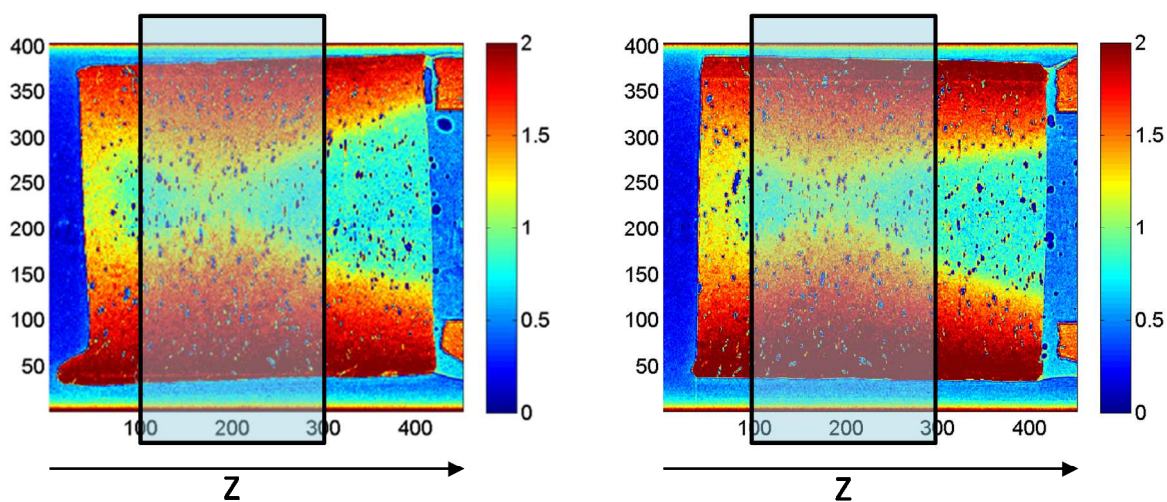

Figure S2. Left and right, orthogonal longitudinal sections through the extrudate near time zero. This shows that there is an uneven impregnation in the Z direction. The units for the colorbar on the right hand are cm^{-1}.

Figure S3 shows the growth of a single particle during the equilibration process. Tentatively, three growth periods can be observed, an initial period of fast rate, followed by a slower period possibly due to agglomeration, followed by a final fast step possibly due to the coalescence of adjacent hotspots.
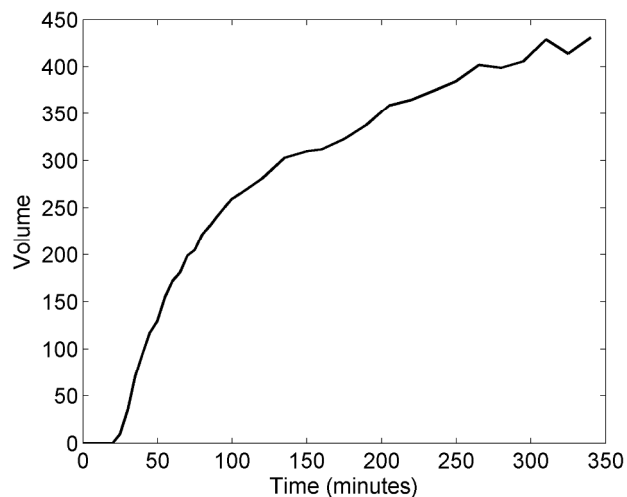
Figure S3. Single particle volume growth of one Al-Mo hotspot in the γ-Al₂O₃ extrudate after incipient wetness impregnation of a 1.3 M [Mo] ammonium heptamolybdate solution at pH 5 as a function of time.
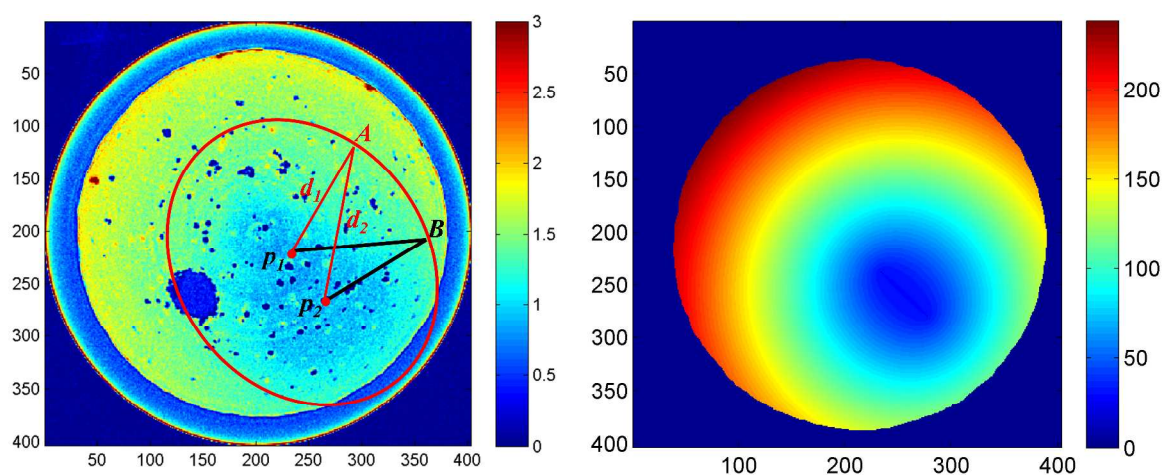

Figure S4. (Left) Slice taken at 60 minutes equilibration illustrating the ellipse defining the diffusion front with foci points P1 and P2 and the hotspots defined at positions A and B; (note units of the colourbar are cm⁻¹). **(Right)** map of the convergence distances (distance from any point to the convergence centre); colorbar in units of number of pixels from the foci points.

The molybdenum diffusion front can be represented as an ellipse that's major and minor axes can be defined by focus points P_1 and P_2, the focus points being equidistant about the centre of the ellipse along the major axis. From the definition of an ellipse the sum of the distances from any point on the ellipse to the two foci is equal to the length of the major axis therefore hotspots A and B are at equivalent distance, convergence distance, CD. As the molybdenum diffuses into the extrudate the ellipse becomes smaller and the convergence distances of A and B become shorter. This convergence distance is used in the subsequent hotspot growth analysis.

$$CD = \left|\left(\frac{d1 + d2}{2}\right)\right|$$

In an ideal system the region of low Mo concentration would be expected at the centre of the extrudate, however in this case it appears that the outer edge of the extrudate was not uniformly exposed to the impregnating solution with the top left hand region being exposed to a greater extent.
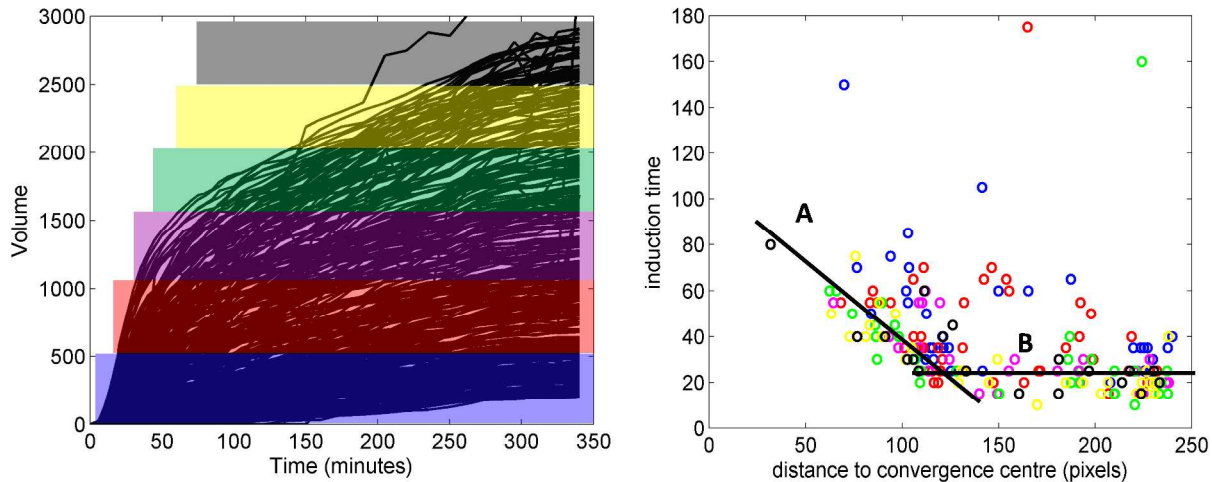

Figure S5. (Left) Volumes of 500 selected particles as a function of time, the colours grouping particles of similar volume. (Right) induction time vs. distance to convergence centre the coloured dots representing particles of similar volume, the colour scheme is based on final volumes as shown in Figure S3 Left.

The data in Figure S5 (Right) appear to follow two trend lines (labeled A and B). Points lying on A indicate that the closer to the convergence centre (where the concentration is lower in the early stages) the longer the induction time. Points lying on line B have a similar induction time which

seems to be independent of convergence distance, being at a point where the concentration of Mo is most likely above a critical value. The data points marked in blue show that for smaller particles there is less correlation between induction time and convergence distance.
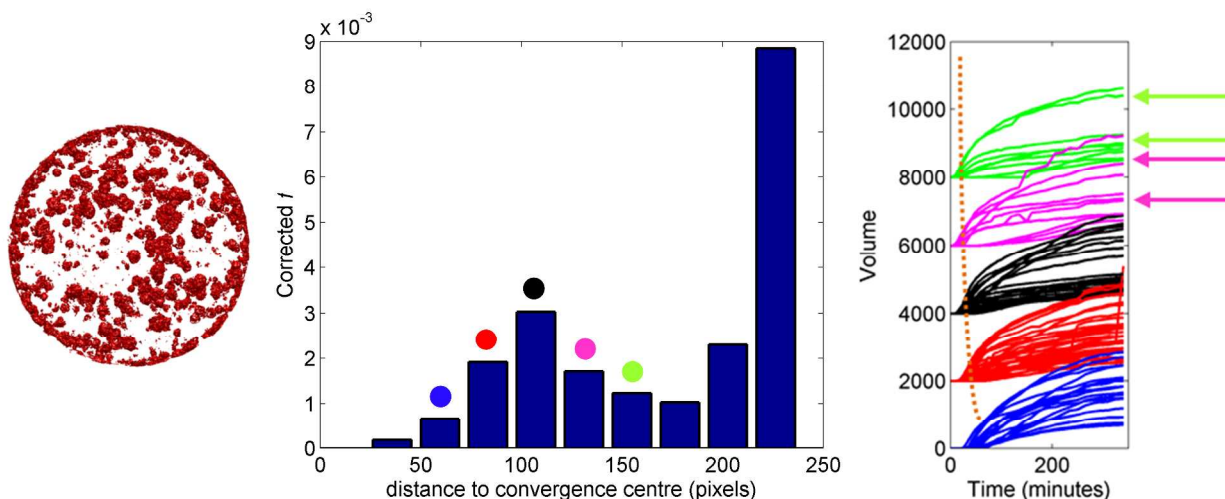

Figure S6   (Left) segmented projection down the cylindrical axis showing distribution of hotspots, the distribution resembles the corrected frequency histogram for the distance to the convergence centre for the 500 selected particles (middle).   (Right) These 500 particles have been grouped according to distance from the convergence centre as indicated by the colours in the histogram (middle).

The volume profiles (Figure S6 (Right)) are colour coded as a function of distance to the convergence centre and offset vertically in each case by 2000 units. The colour codes relate to the components from the histogram in Figure S6 (middle) so that the particles are grouped according to distance from the convergence centre. Particles with final volumes < 500 pixels^3 were excluded. By far, the highest frequency of particle growth is found at the periphery of the extrudate (Figure S6 (middle)) where contact with the impregnating solution is highest. There appears to be no correlation between particle volume and distance to the convergence centre, with particles of all sizes being found in each region. Induction time however, does appear to correlate to convergence distance with longer induction times being observed for particles growing closer to the convergence centre. This trend is depicted by the orange line in Figure S5 (Right) and would imply a minimum concentration of Mo is required for particle growth. In

addition, a bimodality of particle growth is observed, seemingly more apparent at greater distance from the convergence centre, as indicted by the arrows, with larger particles growing faster and small particles having a slower initial growth rate.

Three factors describing particle growth can be concluded from the analysis. Firstly, increasing induction time for particle growth is observed for particles closer to the convergence centre where initial Mo concentration is low. This would indicate that nucleation is dependent on the concentration of molybdenum and therefore is a function of the diffusion of the impregnating solution. This is implicit in the stoichiometry of Equation 1 where a 6:1 ratio of Mo:Al is needed to form the Al-Mo heteropolyanion. However, particle growth is not observed to be concentration dependent, with particles of varying size observed to grow in all regions of the extrudate.

$$12 \, Mo_7O_{24}{}^{6-} + 7 \, Al_2O_3 + 27 \, H_2O + 30 \, H^+ \rightarrow 14Al(OH)_6Mo_6O_{18}{}^{3-} \tag{1}$$
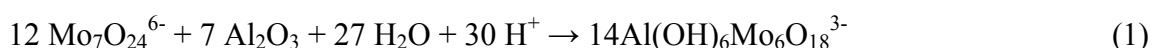
Secondly, Oswald ripening phenomena is not observed, as particle growth appears to be continuous.[1] Of the ~500 particles analysed all are observed to grow continually in size; smaller particles are not observed to dissolve whilst larger particles grow. Thirdly, the majority of particles are found at the periphery of the extrudate, presumably due to higher contact with the impregnating solution. Bridges have been observed to form between hotspots found at the periphery of the extrudate. However, these and other particles which were subject to coalescence were excluded from the analysis. Furthermore, there is some evidence of a temperature effect, as heating by the laser appeared to prompt the faster evolution of Al-Mo hotspots, being observed 15 minutes earlier in the DORS measurements compared to the μ-CT analysis.

---

[1] A. K. Datye, Q. Xu, K. C. Kharas, J. M. McCarty, *Catal. Today.,* 2006, **111**, 59–67